KANONAITE FROM THE METAMORPHIC SOLE OF THE OMAN OPHIOLITE: EVIDENCE FOR HIGH-$f(O_2)$ CONDITIONS DURING RETROGRADE METAMORPHISM

Yaso KUGIMIYA[§], Susumu UMINO and Toshiaki MASUDA

Institute of Geosciences, Shizuoka University, Shizuoka 422-8529, Japan

Yasushi MATSUDA

Department of Life Science, Himeji Institute of Technology, Kamigori-cho, Hyogo 678-1297, Japan

Abstract

Kanonaite has been discovered in a metachert pebble derived from the metamorphic sole of the Oman ophiolite in United Arab Emirates. The kanonaite rims (50 μm in maximum width) manganian andalusite with a distinct chemical discontinuity, and is also found intergrown with muscovite. It contains up to 65 mol.% $Mn^{3+}AlSiO_5$, and the Fe analogue, $Fe^{3+}AlSiO_5$, typically accounts for 3–12 mol.% of the total. Petrographic features suggest that kanonaite formed by reaction between manganian andalusite and quartz, with the addition of K introduced by an aqueous fluid, according to: $6(Al_{0.62}Mn^{3+}_{0.30}Fe^{3+}_{0.08})AlSiO_5 + 3SiO_2 + 2K^+ + 3H_2O \rightarrow 3(Mn^{3+}_{0.60}Al_{0.36}Fe^{3+}_{0.04})AlSiO_5 + K_2(Al_{3.64}Fe^{3+}_{0.36})(Si_6Al_2)O_{20}(OH)_4 + 2H^+$. The formation of kanonaite can be attributed to a retrograde hydration event under high-$f(O_2)$ buffering according to the solid–solid reactions: $14Mn_2O_3 + 4SiO_2 = 4Mn_7SiO_{12} + O_2$ and $Mn_2O_3 + SiO_2 + Al_2SiO_5 = 2MnAlSiO_5$. The formation of kanonaite suggests that the retrograde metamorphism in the sole of the Oman ophiolite involved localized conditions of high $f(O_2)$.

Keywords: kanonaite, manganian andalusite, high fugacity of oxygen, metamorphic sole, Oman ophiolite, United Arab Emirates.

Sommaire

Nous avons trouvé la kanonaïte dans un caillou de métachert dérivé de la base métamorphique de l'ophiolite d'Oman, dans les Émirats arabes unis. La kanonaïte se présente en liseré 50 μm en largeur maximale sur l'andalousite manganifère, avec une discontinuité distincte en composition; elle est aussi en intercroissance avec la muscovite. Elle contient jusqu'à 65% $Mn^{3+}AlSiO_5$ et 3–12% de l'analogue ferrique, $Fe^{3+}AlSiO_5$ (en termes molaires). D'après les aspects pétrographiques, la kanonaïte se serait formée par réaction entre l'andalousite manganifère et le quartz, avec addition de potassium par le biais d'une phase aqueuse: $6(Al_{0.62}Mn^{3+}_{0.30}Fe^{3+}_{0.08})AlSiO_5 + 3SiO_2 + 2K^+ + 3H_2O \rightarrow 3(Mn^{3+}_{0.60}Al_{0.36}Fe^{3+}_{0.04})AlSiO_5 + K_2(Al_{3.64}Fe^{3+}_{0.36})(Si_6Al_2)O_{20}(OH)_4 + 2H^+$. La formation de la kanonaïte serait due à un événement de rétrogression hydratante sous conditions de fugacité élevée d'oxygène, avec tamponage selon les réactions solide–solide: $14Mn_2O_3 + 4SiO_2 = 4Mn_7SiO_{12} + O_2$ et $Mn_2O_3 + SiO_2 + Al_2SiO_5 = 2MnAlSiO_5$. D'après la formation de la kanonaïte, le métamorphisme rétrograde dans la sole du complexe ophiolitique d'Oman a impliqué des conditions locales de $f(O_2)$ élevée.

(Traduit par la Rédaction)

Mots-clés: kanonaïte, andalousite manganifère, fugacité élevée de l'oxygène, sole métamorphique, ophiolite d'Oman, Emirats arabes unis.

Introduction

Manganic minerals in rocks are rare in nature, primarily because the formation and preservation of such sedimentary, diagenetic, or metamorphic manganese-bearing rocks requires high redox potentials. The presence of Mn-bearing minerals can be utilized as a potential tool in determining the fugacity of oxygen, $f(O_2)$, at the time of formation. Members of the manganian andalusite – kanonaite series have been reported from more than twenty localities, but the conditions of formation and the phase relations of kanonaite are still unclear. Few investigations have been made of occurrences in nature (Vrana *et al.* 1978, Kramm 1979) and its stability in experiments (Abs-Wurmbach *et al.* 1983, Abs-Wurmbach & Peters 1999).

[§] *E-mail address*: ykugimiya@yahoo.com

Here, we report a new occurrence of kanonaite from the metamorphic sole beneath the Oman ophiolite in the Bani Hamid area of the United Arab Emirates. The data provide new insight into the overall compositional variation in the andalusite–kanonaite solid solution in manganic metamorphic rocks. We infer the metamorphic conditions at which kanonaite formed in the Bani Hamid metamorphic sole, and explore the implications with regard to $f(O_2)$ conditions.

BACKGROUND INFORMATION

Stability relations in the system Mn–Al–Si–O, especially those involving Mn^{3+}-for-Al substitution in Al_2SiO_5 polymorphs, are strongly dependent on P–T–$f(O_2)$ conditions (Abs-Wurmbach *et al.* 1983). Kanonaite, $Mn^{3+}AlSiO_5$ (Vrana *et al.* 1978), is an end member of the andalusite group, and has been reported in metamorphic sequences in association with manganese-rich quartz schists and metapelites (Vrana *et al.* 1978, Kramm 1979). Previous studies have focused on the formation of manganian andalusite and the miscibility in the system andalusite–kanonaite (Abs-Wurmbach & Langer 1975, Vrana *et al.* 1978, Kramm 1979, Abs-Wurmbach *et al.* 1981, 1983). A solid solution from zero to about 46 mol.% $MnAlSiO_5$ has been demonstrated in the laboratory, and kanonaite has been synthesized with a maximum of 86 mol.% $MnAlSiO_5$ in a few runs below 500°C and 0.3 GPa under the $AgMnO_4$ or PtO_2 internal buffer (Abs-Wurmbach *et al.* 1983). These authors concluded that kanonaite is only stable at temperatures below 500°C and at low fluid pressure. Abs-Wurmbach & Peters (1999), however, synthesized kanonaite at 600°C at 0.4 GPa and along the $MnO_2–Mn_2O_3$ buffer. In nature, the solid solution is continuous up to 79 mol.% $MnAlSiO_5$ and crystallizes at low temperature and pressure along the $MnO_2–Mn_2O_3$ buffer curve (Kramm 1979).

GEOLOGICAL SETTING

The metamorphic sole associated with the Oman Ophiolite is divided into ordinary and extraordinary parts (Gnos & Kurz 1994, Gnos & Nicolas 1996). The ordinary metamorphic sole outcrops sporadically as small slices of no more than a few hundred meters thick over the whole extent of the Oman Ophiolite in the United Arab Emirates (UAE) and the Sultanate of Oman (Fig. 1). The formation of the ordinary metamorphic sole has been regarded as the result of sub-ophiolite metamorphism during intraoceanic thrusting and associated heat-flow from the overriding young and "hot" lithosphere during the late Cretaceous (Searle & Malpas 1980, Boudier & Coleman 1981, Ghent & Stout 1981, Gnos & Kurz 1994, Gnos & Nicolas 1996, Hacker & Mosenfelder 1996). The ordinary metamorphic sole is characterized by a strong inverted thermal gradient of

more than 1°C per meter (Ghent & Stout 1981, Hacker & Mosenfelder 1996), and consists of metabasites and metacherts, including manganese-bearing metasediments (Allemann & Peters 1972, Glennie *et al.* 1974, Ghent & Stout 1981, Searle & Malpas 1980, Kickmaier & Peters 1991, Gnos 1992, Gnos & Peters 1995, Gnos *et al.* 1996). The ordinary metamorphic sole also includes minor amounts of metapelites and marbles, which were metamorphosed under amphibolite- to granulite-facies conditions (Searle & Malpas 1980, Ghent & Stout 1981, Hacker & Mosenfelder 1996).

The metamorphic sole in the Bani Hamid area forms part of the extraordinary metamorphic sole. It occurs as a sheet of up to 2 km in thickness, and occupies an extraordinary position enclosed by peridotite (Gnos & Kurz 1994) near the northern end of the Oman ophiolite (Fig. 1). This extraordinary metamorphic sole is devoid of any strong thermal gradient across the metamorphic sequence, and the whole sequence is considered to have undergone granulite-facies metamorphism (Gnos & Kurz 1994). The extraordinary metamorphic sole thus was emplaced in its present position at an early stage of the intraoceanic thrusting event, and was heated from the hot peridotite walls on both sides (Gnos & Nicolas 1996). The estimated conditions of peak metamorphism for the extraordinary metamorphic sole are 800–850°C at 0.65–0.9 GPa (Gnos & Kurz 1994). The extraordinary metamorphic sole underwent hydration during cooling, associated with decompression (Gnos & Kurz 1994). Retrograde alteration is clearly indicated by the widespread presence of muscovite in quartz-rich lithologies (Gnos & Kurz 1994). Estimated conditions involve a wide range of temperature (700–200°C) and low pressure (<0.4 GPa), and range from lower-amphibolite facies to greenschist-facies conditions (Gnos & Kurz 1994).

Manganian andalusite has been reported from a metachert in the Bani Hamid area (Gnos 1992, Abs-Wurmbach & Peters 1999). The manganian andalusite in this area is found as a stable phase at the granulite facies and partly at the amphibolite-facies conditions of retrograde metamorphism (Gnos 1992). We found kanonaite in two pebbles of metachert from the extraordinary metamorphic sole in the Bani Hamid area (Fig. 1).

PETROGRAPHY AND MINERAL CHEMISTRY

The chemical composition of minerals was established by wavelength-dispersion X-ray microanalysis (JCXA733, JEOL) at Shizuoka University. Elemental color maps were produced using a similar microanalyzer (JXA8800M, JEOL) at the Himeji Institute of Technology. Correction procedures follow the method of Bence & Albee (1968). Representative results of spot analyses are given in Table 1 and 2, and element maps are shown in Figure 2.

The kanonaite- and manganian-andalusite-bearing metachert consists primarily of quartz with subordinate amounts of manganian andalusite, plagioclase and muscovite, and minor amounts of kanonaite, manganian hematite, braunite, clinochlore, biotite and apatite. The samples are light gray in color and have a weak wavy foliation defined by parallel arrangement of muscovite and biotite flakes. The constituent minerals were divided into assemblages of primary and secondary minerals based on petrographic observations of textures in sample BH7. The primary minerals are quartz, K-feldspar, manganian andalusite, manganian hematite, muscovite, biotite and clinochlore, whereas the secondary minerals are muscovite, kanonaite, braunite, clinochlore and albite. The primary minerals are usually larger (up to 0.9 mm) than the secondary minerals and have accordion shapes with wavy foliation due to plastic deformation, whereas the secondary minerals have shapes characteristic of aggregates and symplectitic static growth. The sample is slightly altered, and K-feldspar is partly replaced by albite + epidote.

Kanonaite exhibits a deep emerald-green to deep golden yellow pleochroism under the microscope (Figs. 2a, b), with birefringence of first-order yellow to second-order green. It occurs as a rim on manganian andalusite grains, with a maximum rim width of 50 μm. The contact between kanonaite and manganian andalusite is sinuous and discontinuous in terms of Mn content (Fig. 2c). The elemental maps of Mn and Al (Figs. 2c, d) reveal that the distribution of these elements is homogeneous. The rim locally attains a $MnAlSiO_5$ content of about 65 mol.% (Table 1, Fig. 3). A chemical profile through the manganian andalusite and kanonaite is shown in Figure 4. The occurrence of anastomosing muscovite in the manganian andalusite was not observed in the kanonaite (Figs. 2e, 5). Kanonaite is commonly intergrown with muscovite (Fig. 5).
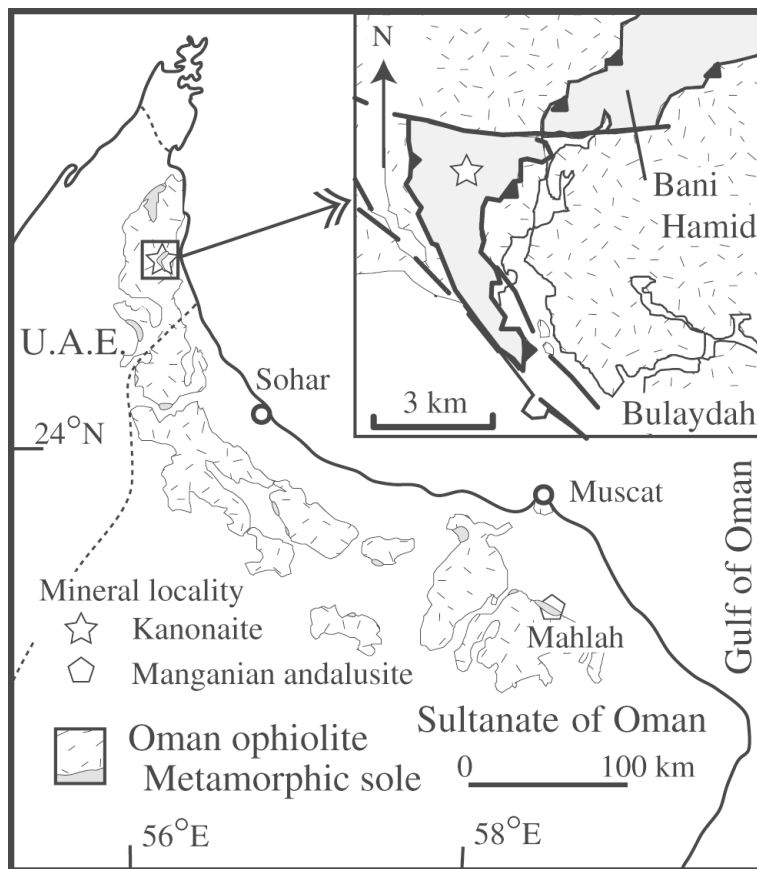

FIG. 1. Geological outline of the Oman ophiolite and its metamorphic sole, after Lippard et al. (1986), showing the occurrence of kanonaite and manganian andalusite.
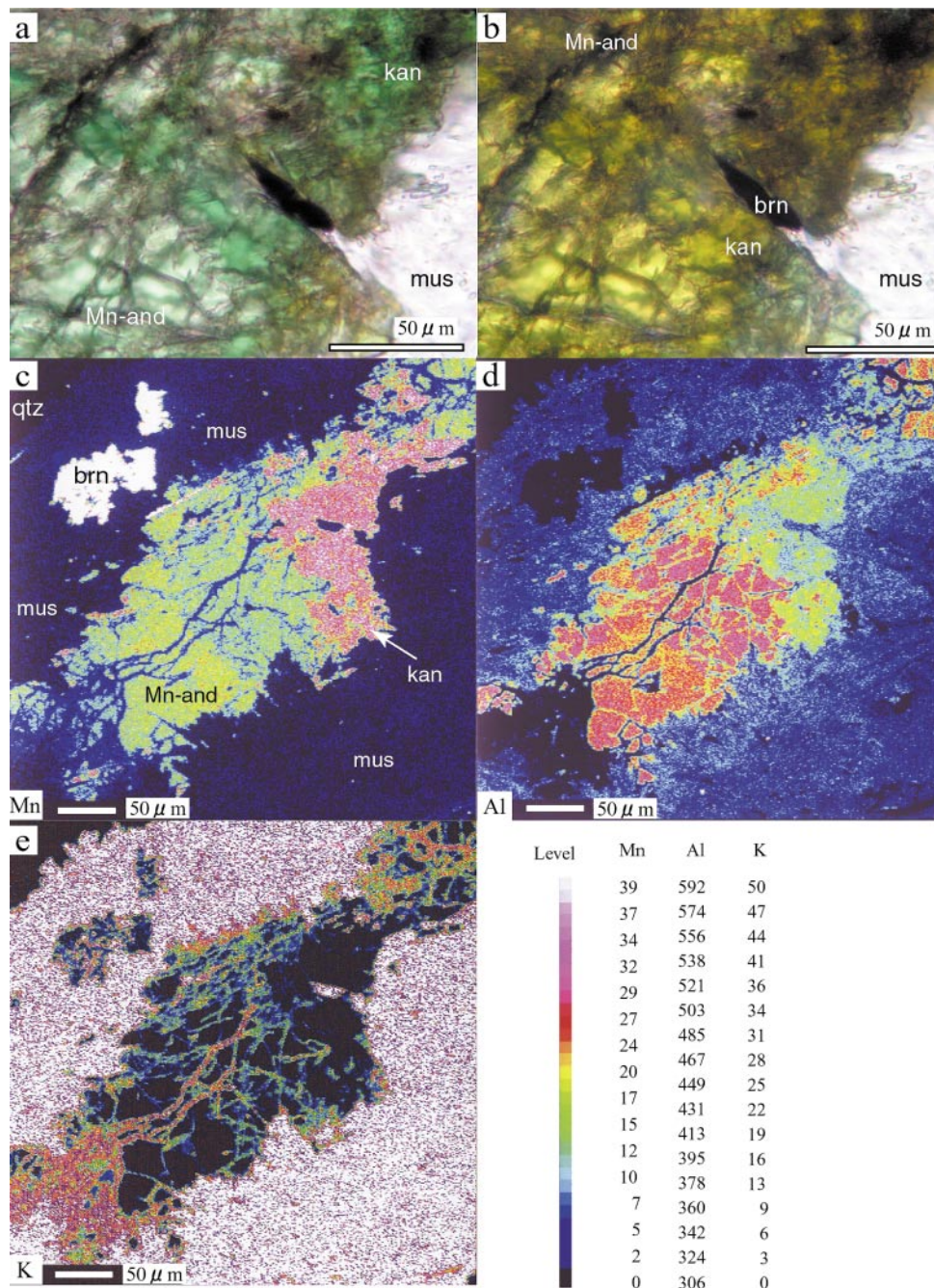
Fig. 2.   Occurrence of kanonaite and manganian andalusite in metachert in the Bani Hamid area. Photomicrographs (a) and (b) show pleochroism of kanonaite (deep golden yellow to deep emerald-green) and manganian andalusite (golden yellow to emerald-green) under plane-polarized light; lower polar of (b) is rotated 90° from (a). (c)–(e) Element-distribution maps showing Mn, Al and K, respectively. Lighter colors indicate higher concentrations of elements. In (c), the pink area is kanonaite (up to 65 mol.% kanonaite), the pale green area is manganian andalusite (32 mol.% kanonaite). (d) Element-distribution map of Al showing Mn^{3+}–Al substitution in kanonaite and manganian andalusite. (e) Element-distribution map of K. Manganian andalusite is enclosed and cut by muscovite aggregates. Kanonaite is intergrown with muscovite. Minerals abbreviations: kan, kanonaite; Mn-and, manganian andalusite; mus, muscovite; brn, braunite; qtz, quartz.
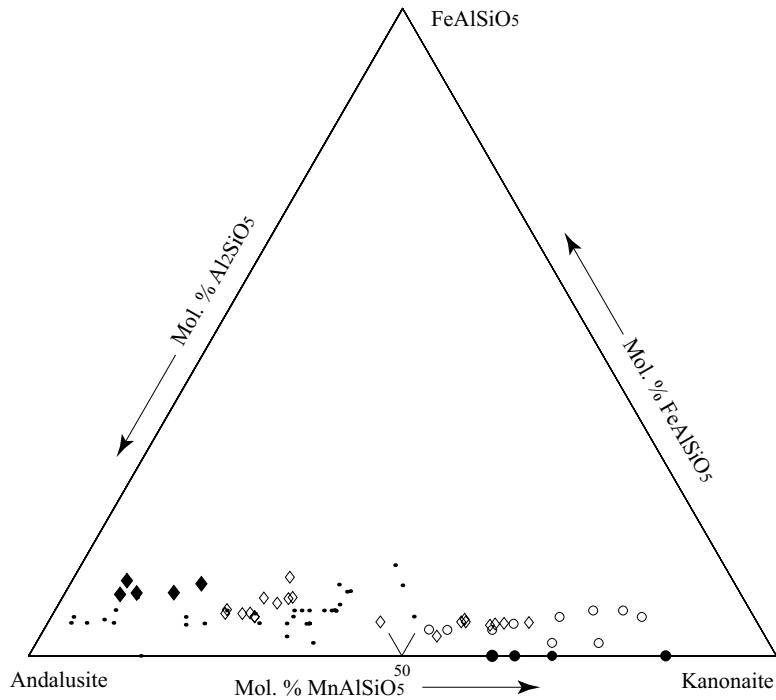
Fig. 3. AlAlSiO$_5$–MnAlSiO$_5$–FeAlSiO$_5$ diagram. Open diamonds: this study; open circles: Vrana *et al.* (1978), Kramm (1979) and Smith *et al.* (1982) for kanonaite; solid circle: Abs-Wurmbach *et al.* (1983) and Abs-Wurmbach & Peters (1999) for synthesized kanonaite; solid diamonds: Gnos (1992), and solid dots: Bäckström (1896), Klemm (1911), Ödman (1950), Prider & Wheeler, H.W (1960), Suzuki *et al.* (1965), Herbosch (1968), Meinhold & Frisch (1970), Kramm (1973), Abraham & Schreyer (1975), Grapes & Hashimoto (1978), Smith *et al.* (1982), Basu & Mruma (1985), Grambling & Williams (1985) for manganian andalusite.
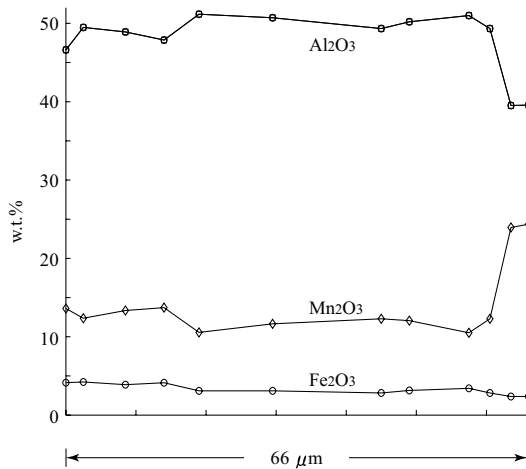

Fig. 4. Chemical profile over manganian andalusite and kanonaite composite in Figure 5. Plotted data are shown in Table 1.

Manganian andalusite also exhibits emerald-green to golden yellow pleochroism (Figs. 2a, b) and the birefringence is similar to that of kanonaite. It usually occurs as prismatic crystals of 0.3–0.4 mm in width and 0.5–0.9 mm in length. The rim is partially replaced with aggregates of fine flakes of muscovite. The Mn content of the rim of the manganian andalusite coexisting with muscovite aggregates is variable (Fig. 2c). The MnAlSiO$_5$ content of most grains is 22–30 mol.% (Table 1, Fig. 3).

Muscovite occurs as aggregates, intergrown with kanonaite surrounding manganian andalusite (Fig. 2e) and matrix flakes (Table 2). Muscovite may also occur as a columnar pseudomorph after manganian andalusite, yet usually contains less than 1 wt% Mn$_2$O$_3$ (Table 2). No chemical trends are developed in such muscovite (Table 2). Biotite flakes contain up to 3.4 wt% Mn$_2$O$_3$, but are not found in the vicinity of the manganian andalusite. Hematite grains are spherical in shape and contain less than 3 wt% Mn$_2$O$_3$ (Table 2, Fig. 5). Braunite is associated with the muscovite aggregates and shows

an amoeboid shape (Table 2, Fig. 5). No isolated braunite occur in the thin section. Clinochlore occurs locally in muscovite aggregates (Fig. 5). Potassium feldspar has the composition of $An_{10}Ab_{49}Or_{41}$ at the core and An_4Ab_{96} at the rim. Quartz grains exhibit a weak undulatory extinction with irregular grain-boundaries and many healed cracks, indicated by arrays of undifferentiated fine inclusions.

DISCUSSION

Formation of kanonaite and manganian andalusite

The manganian andalusite in the metacherts is considered to have formed during granulite-facies condi-

tions (Gnos 1992), whereas the kanonaite is considered to have formed during retrograde metamorphism on the basis of petrographic observations of texture (Figs. 2 and 5).

The textures seen in back-scattered electron images indicate that the intergrowth of kanonaite with muscovite occurred after the formation of manganian andalusite (Fig. 5). This intergrowth was induced by hydration during retrograde metamorphism. As kanonaite grains are closely associated with intergrown muscovite, the following manganese-release retrograde reaction seems reasonable:

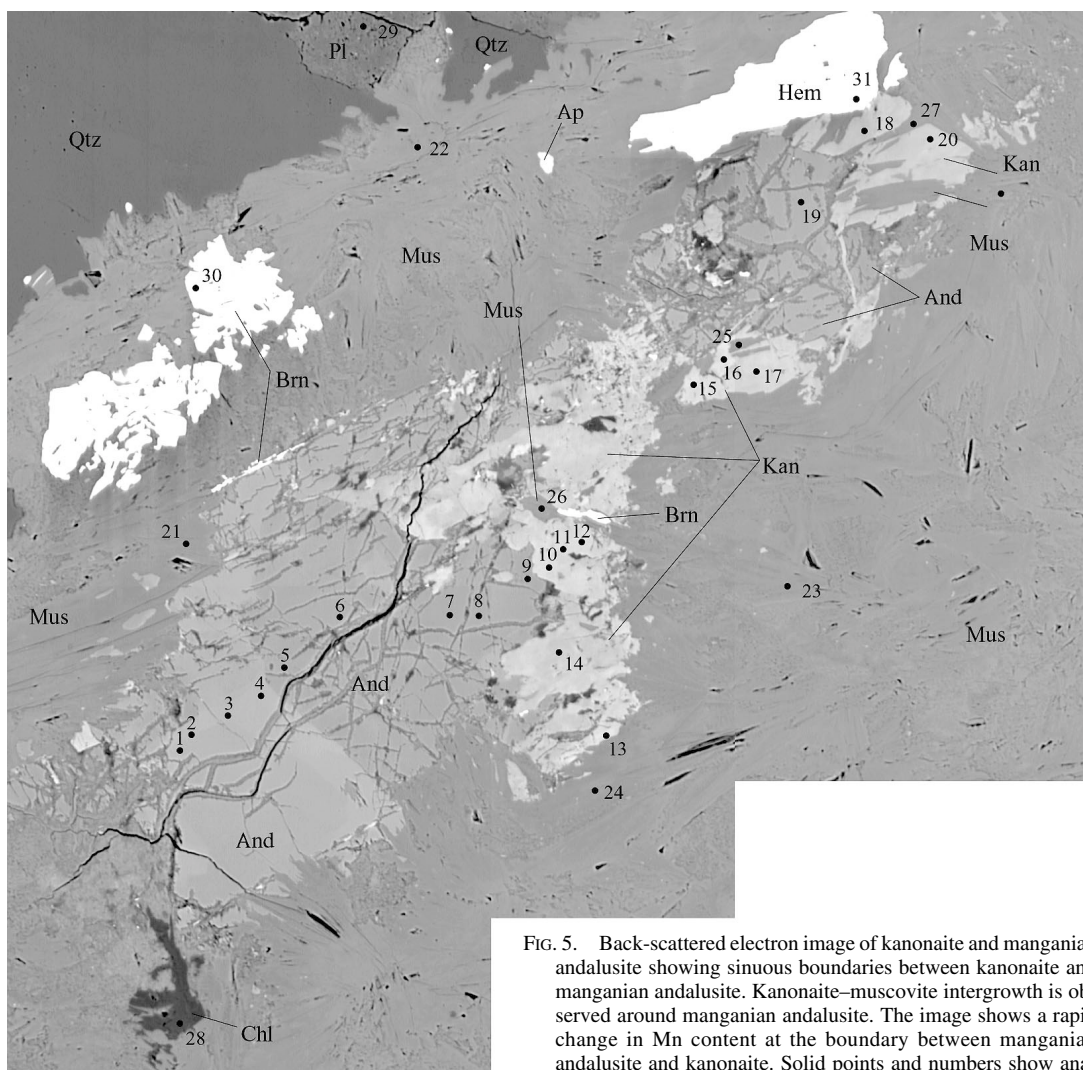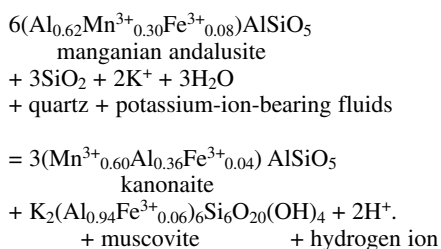FIG. 5.   Back-scattered electron image of kanonaite and manganian andalusite showing sinuous boundaries between kanonaite and manganian andalusite. Kanonaite–muscovite intergrowth is observed around manganian andalusite. The image shows a rapid change in Mn content at the boundary between manganian andalusite and kanonaite. Solid points and numbers show analytical points and numbers in Tables 1 and 2.

TABLE 1. COMPOSITION OF KANONAITE AND MANGANIAN ANDALUSITE, OMAN OPHIOLITE

No.	And 1	And 2	And 3	And 4	And 5	And 6	And 7	And 8	And 9	And 10	Kan 11	Kan 12	Kan 13	And 14	Kan 15	Kan 16	Kan 17	Kan 18	And 19	Kan 20
SiO_2 wt%	34.63	34.10	34.60	34.33	35.97	34.09	35.84	34.71	35.06	35.84	33.59	33.66	33.00	34.03	33.01	33.23	32.84	32.58	34.13	33.87
Al_2O_3	46.61	49.48	48.91	47.87	51.17	50.72	49.33	50.20	51.00	49.33	39.51	39.56	37.34	43.76	38.83	40.04	38.32	37.77	47.22	41.13
Fe_2O_3*	4.14	4.23	3.88	4.13	3.09	3.10	2.82	3.14	3.41	2.82	2.37	2.38	2.34	2.41	2.15	2.59	2.24	2.24	5.69	1.38
Mn_2O_3**	13.61	12.36	13.35	13.72	10.55	11.65	12.29	12.05	10.50	12.29	23.95	24.36	28.16	19.82	25.98	24.46	26.03	26.42	12.93	23.35
MgO	n.d.	n.d.	n.d.	n.d.	n.d.	n.d.	n.d.	n.d.	n.d.	n.d.	n.d.	n.d.	n.d.	n.d.	n.d.	n.d.	n.d.	n.d.	0.13	n.d.
Total	98.99	100.17	100.75	100.20	100.78	99.55	100.27	100.10	100.17	100.27	99.42	99.97	100.84	100.02	99.97	100.32	99.42	99.01	100.10	99.74
Si *apfu*	1.007	0.977	0.987	0.987	1.011	0.976	1.018	0.989	0.994	1.018	1.005	1.003	0.989	0.996	0.990	0.988	0.991	0.990	0.986	1.004
Al	1.598	1.670	1.644	1.623	1.695	1.711	1.651	1.686	1.703	1.651	1.394	1.390	1.319	1.510	1.372	1.404	1.363	1.352	1.607	1.437
Fe^{3+}	0.091	0.091	0.083	0.089	0.065	0.067	0.060	0.067	0.073	0.060	0.053	0.053	0.053	0.053	0.049	0.058	0.051	0.051	0.124	0.031
Mn^{3+}	0.307	0.274	0.295	0.306	0.229	0.257	0.269	0.265	0.230	0.269	0.552	0.559	0.649	0.446	0.599	0.560	0.604	0.617	0.291	0.530
Mg																			0.006	
Total	3.003	2.990	2.996	2.999	2.999	2.987	2.997	2.996	3.002	2.997	3.004	3.005	3.000	3.002	2.999	2.999	3.000	2.999	3.000	3.002
$FeAlSiO_5$	9.1	9.0	8.2	8.9	6.6	6.6	6.1	6.7	7.2	6.1	5.3	5.3	5.2	5.3	4.8	5.7	5.0	5.1	12.2	3.1
$AlAlSiO_5$	60.2	64.1	62.6	60.8	70.4	68.2	66.8	67.1	69.8	66.8	39.5	38.9	30.5	50.3	35.9	38.8	35.1	33.9	58.9	43.9
$MnAlSiO_5$	30.8	27.0	29.1	30.3	23.0	25.3	27.2	26.3	22.9	27.2	55.2	55.8	64.3	44.4	59.3	55.4	59.9	61.1	28.8	53.1

Symbols: And: manganian andalusite; Kan: kanonaite; the elements Ti, Ca, Na, K, and Cr were not detcted in kanonaite and manganian andalusite.
* Total Fe as Fe_2O_3, ** total Mn as Mn_2O_3, n.d.: not determined. Representative results of electron-microprobe analyses, sample BH7, recalculated on the basis of five oxygen atoms per formula unit. Columns 13 and 14, 18 and 19: juxtaposed kanonaite and andalusite.

$$6(Al_{0.62}Mn^{3+}_{0.30}Fe^{3+}_{0.08})AlSiO_5$$
manganian andalusite
$$+ 3SiO_2 + 2K^+ + 3H_2O$$
+ quartz + potassium-ion-bearing fluids

$$= 3(Mn^{3+}_{0.60}Al_{0.36}Fe^{3+}_{0.04}) AlSiO_5$$
kanonaite
$$+ K_2(Al_{0.94}Fe^{3+}_{0.06})_6Si_6O_{20}(OH)_4 + 2H^+.$$
+ muscovite   + hydrogen ion

One likely possibility for the source of potassium ions in the infiltrating fluids is the substitution of Na^+ for K^+, as the rim of the K-feldspar is more sodic (Table 2). This reaction is supported by the observation of widespread low-temperature hydrothermal alteration in the metamorphic sole in the Oman ophiolite by several earlier investigators (*e.g.,* Searle & Malpas 1980, Ghent & Stout 1981, Hacker & Mosenfelder 1996, Gnos & Nicolas 1996). Infiltration of externally derived fluids, either meteoric water or fluid from other low-grade metamorphic assemblages, may have penetrated along the thrust plane during the late or post-emplacement movements of the ophiolite. This inference is supported by the restriction of low-grade deformation and alteration to the shear zone separating the Bani Hamid metamorphic rocks and the ophiolite suite (Gnos & Nicolas 1996).

The columnar pseudomorph of muscovite after manganian andalusite and the undulatory extinction of quartz in the matrix imply that deformation during kanonaite formation was not significant, although strong deformation during the thrusting of the ocean floor is

expected (*e.g.,* Hacker & Mosenfelder 1996, Hacker *et al.* 1996). Thus, kanonaite must have formed below the brittle-to-plastic transition temperature of quartz, that is, below 250°C (*e.g.,* Passchier & Truow 1996). This estimated temperature for the formation of kanonaite, however, is too low compared with the conditions of retrograde metamorphism in the Bani Hamid area (Gnos & Kurz 1994). The absence of pyrophyllite indicates that the breakdown temperature of manganian andalusite must have been above 300°C (at 0.4 GPa), at which temperature the reaction: pyrophyllite + braunite + pyrolusite from manganian andalusite + quartz + H_2O would be expected (Abs-Wurmbach *et al.* 1983). The presence of albite and the absence of paragonite adjacent to the pseudomorphs of manganian andalusite indicate that the limiting reaction on the high-temperature side is albite + manganian andalusite + H_2O = paragonite + quartz + bixbyite (500–550°C at 0.4 GPa). The assemblage muscovite + clinochlore in muscovite aggregates must have formed below the amphibolite facies (*e.g.,* Spear 1993). Kanonaite formed at the expense of manganian andalusite can be bracketed in the temperature range of 300–550°C. This is in agreement with natural occurrences of kanonaite reported from amphibolite-facies metamorphic rocks (Vrana *et al.* 1978) and the experimental results showing kanonaite to be stable only between 400 and 600°C (Abs-Wurmbach *et al.* 1983, Abs-Wurmbach & Peters 1999).

Previous reports on the natural occurrences (Table 3, Fig. 3) suggest that kanonaite forms at metamorphic conditions less than 400°C at 0.1–0.2 GPa (Kramm 1979) and at the staurolite–almandine subfacies of the

amphibolite facies, at about 550–650°C under conditions of high oxygen fugacity (Vrana *et al.* 1978). Kramm (1979) explained that kanonaite in low-grade manganese-bearing sediments at Salm-Château, Belgium, was produced during the introduction of Mn released from manganian hematite *via* a solution to rocks containing manganian andalusite under the MnO_2–Mn_2O_3 buffer curve. He concluded that kanonaite formed below 400°C because of the presence of kaolinite and paragonite but absence of feldspar in association with kanonaite. That occurrence likely formed at a lower temperature than the kanonaite of this study. Petrographic observation of kanonaite + muscovite intergrowth in the sample BH7 indicates that the Mn in kanonaite is derived from manganian andalusite breakdown reaction even if the Mn–Al exchange reaction is also likely to occur easily between manganian hematite and manganian andalusite (Fig. 5).

Implications for f(O₂) conditions during retrograde metamorphism

The reason for the scarcity of kanonaite when compared to manganian andalusite remains unclear. One explanation could be that kanonaite forms only under higher $f(O_2)$ conditions than manganian andalusite, as shown in Figure 6. Higher levels of the kanonaite component could be achieved at very high $f(O_2)$ conditions above the MnO_2–Mn_2O_3 buffer curve (Kramm 1979). The kanonaite- and manganian-andalusite-bearing samples could also be derived from manganic sediments and their metamorphic equivalents, because these rocks may have remained under conditions of high $f(O_2)$ from the start of sedimentation through to high-temperature metamorphism (Grapes & Hashimoto 1978). The occurrence of piemontite + quartz veins in the Mahlah area,

TABLE 2. COMPOSITION OF MINERALS ASSOCIATED WITH KANONAITE AND MANGANIAN ANDALUSITE, OMAN OPHIOLITE

Sample No.	Ms aggre. 21	Ms aggre. 22	Ms aggre. 23	Ms aggre. 24	Ms int. 25	Ms int. 26	Ms int. 27	Ms matrix 167	Ms matrix 168	Bt matrix z48	Chl aggre. 28	Chl matrix 2.3	Ab 29	Bnt 30	Hem 31
SiO_2 wt%	46.25	46.88	45.97	45.14	46.12	46.42	44.31	46.54	47.32	39.13	29.62	28.14	66.84	10.20	0.23
TiO_2	n.d.	n.d.	n.d.	n.d.	n.d.	n.d.	n.d.	n.d.	n.d.	1.20	n.d.	n.d.	n.d.	n.d.	1.95
Al_2O_3	34.06	33.02	31.05	32.93	34.88	34.61	34.89	34.85	33.91	19.50	23.55	23.77	20.92	0.98	0.38
Fe_2O_3*	2.41	2.52	2.55	2.91	2.50	2.69	2.36	0.54	1.93	3.63	n.d.	0.80	n.d.	5.96	94.62
MnO**	0.70	0.00	0.87	0.55	0.91	0.52	0.71	0.00	0.46	3.49	1.70	1.70	n.d.	#83.24	#2.48
MgO	0.70	1.52	3.62	2.70	1.10	0.72	1.50	1.43	0.99	19.08	33.10	34.53	n.d.	0.20	n.d.
CaO	n.d.	n.d.	n.d.	n.d.	n.d.	n.d.	n.d.	n.d.	n.d.	n.d.	n.d.	n.d.	0.72	n.d.	n.d.
Na_2O	0.61	0.47	0.40	0.36	0.53	0.46	0.54	0.29	0.44	0.24	n.d.	n.d.	11.02	n.d.	n.d.
K_2O	10.45	11.02	11.22	11.37	9.36	10.53	10.90	11.42	11.10	9.71	n.d.	n.d.	n.d.	n.d.	n.d.
Total	95.17	95.43	95.67	95.95	95.39	95.95	95.21	95.07	96.16	95.97	87.96	88.94	99.50	100.59	99.63
Si *apfu*	6.192	6.261	6.190	6.060	6.127	6.162	5.970	6.206	6.266	5.502	5.468	5.180	2.936	1.026	0.006
^{IV}Al	1.808	1.739	1.810	1.940	1.873	1.838	2.030	1.794	1.734	2.498	2.532	2.820	0.064		
Σ	8.000	8.000	8.000	8.000	8.000	8.000	8.000	8.000	8.000	8.000	8.000	8.000	3.000	1.026	0.006
^{VI}Al	3.566	3.458	3.118	3.271	3.587	3.576	3.511	3.682	3.558	0.734	2.592	2.336	2.915	0.116	0.011
Ti										0.127					0.037
Fe^{3+}	0.243	0.253	0.259	0.294	0.250	0.269	0.240	0.054	0.193	0.384		0.111		0.451	1.818
Mn^{3+}														5.432	0.084
Mn^{2+}	0.080		0.099	0.062	0.102	0.059	0.081		0.052	0.416	0.266	0.264		0.943	0.043
Mg	0.140	0.303	0.726	0.540	0.217	0.143	0.301	0.284	0.195	4.000	9.112	9.476		0.031	0.000
Σ	4.029	4.014	4.202	4.167	4.156	4.046	4.133	4.020	3.997	5.661	11.970	12.187	2.915	6.974	1.994
Ca													0.034		
Na	0.157	0.121	0.103	0.093	0.137	0.117	0.141	0.075	0.114	0.064			0.939		
K	1.784	1.878	1.927	1.948	1.586	1.784	1.873	1.942	1.875	1.741			0.000		
Σ	1.941	2.000	2.031	2.041	1.723	1.901	2.014	2.017	1.989	1.805			0.972		

* Total Fe as Fe_2O_3; ** Total Mn as MnO; # Total Mn as Mn_2O_3; Cr not detected in muscovite, biotite, clinochlore, albite, braunite and hematite. Mn^{3+} and Mn^{2+} in braunite: $Mn^{3+} = 6 - Al - Fe^{3+} - Ti$, $Mn^{2+} = Mn$ total $- Mn^{3+}$; Mn^{3+} and Mn^{2+} in hematite: $Mn^{2+} = Si + Ti$, Mn^{3+} = Mn total $- Mn^{2+}$; n.d.: not determined; aggre.: aggregate. Representative results of electron-microprobe analyses, sample BH7, recalculated on the basis of the following number of oxygen atoms: 22 (muscovite, biotite), 28 (clinochlore), 8 (albite), 12 (braunite) and 4 (hematite). Symbols: Ms: muscovite, Bt: biotite, Chl: clinochlore, Ab: albite, Bnt: braunite, Hem: hematite.

Wadi Tayin, in the southern Oman ophiolite area (Ghent & Stout 1981) also suggests that high-$f(O_2)$ fluids have indeed infiltrated the sole, and conditions of high $f(O_2)$ could have been maintained at high temperatures up until the latest stage of metamorphism.

In the present study, the presence of manganian hematite and braunite indicates buffering on a solid-solid reaction: $Mn_2O_3 + SiO_2 + Al_2SiO_5 = 2MnAlSiO_5$ (pers. commun., E.J. Essene) and a braunite-forming reaction: $14Mn_2O_3 + 4SiO_2 = 4Mn_7SiO_{12} + O_2$. The absense of pyrolusite indicates that the MnO_2–Mn_2O_3 buffer is the upper limit of $f(O_2)$ condition, whereas the absence of spessartine indicates that the Mn_2O_3–Mn_3O_4 buffer curve is the lower limit of $f(O_2)$ conditions of kanonaite (Fig. 6). The braunite-forming reaction indicates that growth of kanonaite occurred at higher $f(O_2)$ conditions than the stability of manganian andalusite. Thus kanonaite should form at a higher $f(O_2)$ – T condition than manganian andalusite during retrograde metamorphism. On the other hand, kanonaite from the metamorphic sole of the Bani Hamid area contains less $MnAlSiO_5$ than the products of synthesis (Fig. 3), which are buffered on a reaction of $14Mn_2O_3 + 4SiO_2 = 4Mn_7SiO_{12} + O_2$. The lower $MnAlSiO_5$ content of our kanonaite might be the result of slightly lower $f(O_2)$ – T conditions than in experiments (Abs-Wurmbach *et al.*

1983, Abs-Wurmbach & Peters 1999). Thus, the $MnAlSiO_5$ content of kanonaite may be a useful monitor of oxygen fugacity during retrograde metamorphism (Fig. 6).

TABLE 3. OCCURRENCES OF KANONAITE: THEIR LOCALITIES, LITHOLOGIES, PROTOLITHS AND GRADE OF METAMORPHISM

Locality	Lithology	Protolith	Metamorphism	Minerals	Refs.
Salm-Château, Belgium	low-grade semi-schist	mangani-ferous phyllite	greenschist facies (?) 1–2 kbar, 360–400°C	And, Sps, Rds, Qtz, Mn-and, Kan	1, 2, 3, 4
Kanona, Zambia	quartzite schist	quartzite	St–Alm subfacies, amphibolite facies	Kan, Gah, Chl, Cor, Qtz, Ky, Ms*, And*	5
Bani Hamid, United Arab Emirates	Mn-rich metachert	mangani-ferous chert	amphibolite to greenschist facies	And*, Kan, Qtz, Ab, Bt, Ms, Brn, Chl, Ap	7, 8, 9, 10

Symbols: And: andalusite, And* manganian andalusite, Kan: kanonaite; Sps: spessartine; Rhs: rhodochrosite; Qtz: quartz; Brn: braunite; Ky: kyanite; Ms: muscovite; Ms*: manganian muscovite; Ab: albite; Ap: apatite; Cor: coronadite, Gah: gahnite, St: staurolite; Alm: almandine. References: (1) Corin (1934), (2) Kramm (1973), (3) Herbosch (1968), (4) Kramm (1979), (5) Vrana *et al.* (1978), (7) Gnos (1992), (8) Gnos & Kurz (1994), (9) Hacker *et al.* (1996), (10) Abs-Wurmbach & Peters (1999).
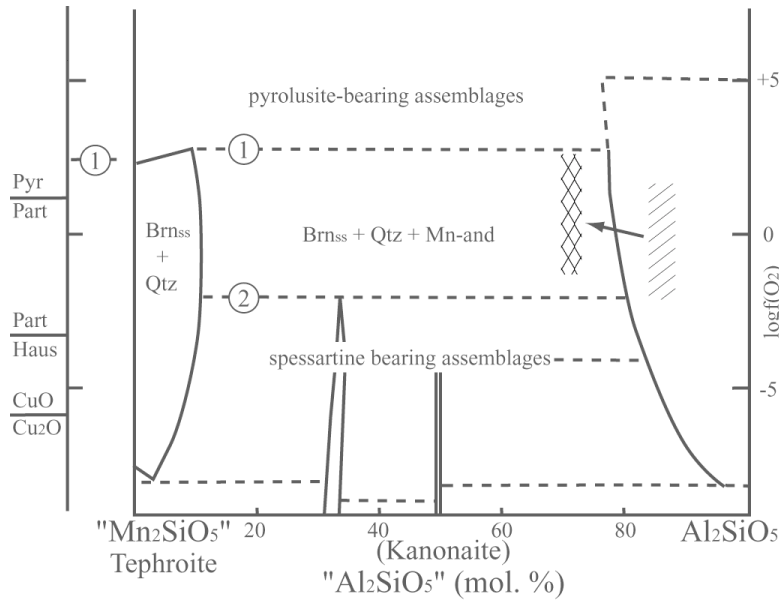

FIG. 6. Stability field of kanonaite and manganian andalusite in the system Mn–Al–Si–O at 600°C and 0.4 GPa, modified after Abs-Wurmbach & Peters (1999). Crosses and shading are possible conditions of $f(O_2)$ for kanonaite- and manganian-andalusite-bearing assemblages in metachert, respectively. Dotted line (1) and (2) show the pyrolusite + quartz = braunite + O_2 reaction and the braunite solid-solution + quartz + manganian andalusite = spessartine + O_2 reaction, respectively.

REFERENCES

ABRAHAM, K. & SCHREYER, W. (1975): Minerals from viridine hornfels from Darmstadt, Germany. *Contrib. Mineral. Petrol.* **49**, 1-20.

ABS-WURMBACH, I. & LANGER, K. (1975): Synthetic Mn^{3+}-kyanite and viridine, $(Al_{2-x}Mn^{3+}_x)SiO_5$, in the system Al_2O_3–MnO–MnO_2–SiO_2. *Contrib. Mineral. Petrol.* **49**, 21-38.

_____, _____ & SCHREYER, W. (1983): The influence of Mn^{3+} on stability relations of the Al_2SiO_5 polymorphs with special emphasis on manganian andalusites (viridines), $(Al_{1-x}Mn^{3+}_x)_2(O/SiO_4)$: an experimental investigation. *J. Petrol.* **24**, 48-75.

_____, _____, SEIFERT, F. & TILLMANNS, E. (1981): The crystal chemistry of (Mn^{3+}, Fe^{3+})-substituted andalusites (viridine and kanonaite), $(Al_{1-x-y}Mn^{3+}_xFe^{3+}_y)_2(O/SiO_4)$: crystal structure refinements, Mössbauer, and polarized optical absorption spectra. *Z. Kristallogr.* **155**, 81-113.

_____ & PETERS, T. (1999): The Mn–Al–Si–O system: an experimental study of phase relations applied to parageneses in manganese-rich ores and rocks. *Eur. J. Mineral.* **11**, 45-68.

ALLEMANN, F. & PETERS, T. (1972): The ophiolite–radiolarite belt of the North-Oman Mountains. *Eclog. Geol. Helv.* **65**, 657-697.

BÄCKSTRÖM, H. (1896): Manganandalusit från Vestanå. *Geol. Fören. Stockholm Förh.* **18**, 386-389.

BASU, N.K. & MRUMA, A.H. (1985): Mineral chemistry and stability relations of talc – piedmontite – viridine bearing quartzite of Mautia Hill, Mpwapwa district, Tanzania, and their similarity with the Konse Series rocks. *Indian J. Earth Sci.* **12**, 223-230.

BENCE, A.E. & ALBEE, A.L. (1968): Empirical correction factors for the electron microanalysis of silicates and oxides. *J. Geol.* **76**, 382-403.

BOUDIER, F. & COLEMAN, R.G. (1981): Cross section through the peridotite in the Samail ophiolite, southeastern Oman Mountains. *J. Geophys. Res.* **86**, 2573-2592.

CORIN, F. (1934): Identité probable de la gosseletite et de la viridine (manganandalousite). Occurrence de la viridine à Salm-Château. *Ann. Soc. Géol. Belgique* **57**, B152-157.

GHENT, E.D. & STOUT, M.Z. (1981): Metamorphism at the base of the Samail ophiolite, southeastern Oman Mountains. *J. Geophys. Res.* **86**, 2557-2571.

GLENNIE, K.W., BOEUF, M.G.A., HUGHES-CLARKE, M.W., MOODY-STUART, M., PILAAR, W.F.H. & REINHARDT, B.M. (1974): Geology of the Oman Mountains. *Ver. Konink. Neder. Geol. Mijn. Genootschap.* **31**, 1-423.

GNOS, E. (1992): *The Metamorphic Rocks Associated with the Semail Ophiolite* (*Sultanate of Oman and United Arab Emirates*). Ph.D. thesis, Univ. of Berne, Berne, Switzerland.

_____, ARMBRUSTER, T. & NYFELER, D. (1996): Kanoite, donpeacorite and tirodite: Mn–Mg-silicates from a manganiferous quartzite in the United Arab Emirates. *Eur. J. Mineral.* **8**, 251-261.

_____ & KURZ, D. (1994): Sapphirine–quartz and sapphirine–corundum assemblages in metamorphic rocks associated with the Semail ophiolite (United Arab Emirates). *Contrib. Mineral. Petrol.* **116**, 398-410.

_____ & NICOLAS, A. (1996): Structural evolution of the northern end of the Oman ophiolite and enclosed granulites. *Tectonophysics* **254**, 111-137.

_____ & PETERS, T. (1995): Tephroite–hausmannite–galaxite from a granulite-facies manganese rock of the United Arab Emirates. *Contrib. Mineral. Petrol.* **120**, 372-377.

GRAMBLING, J.A. & WILLIAMS, M.L. (1985): The effects of Fe^{3+} and Mn^{3+} on aluminum silicate phase relations in north-central New Mexico, U.S.A. *J. Petrol.* **26**, 324-354.

GRAPES, R.H. & HASHIMOTO, S. (1978): Manganiferous schists and their origin, Hidaka Mountains, Hokkaido, Japan. *Contrib. Mineral. Petrol.* **68**, 23-35.

HACKER, B.R. & MOSENFELDER, J.L. (1996): Metamorphism and deformation along the emplacement thrust of the Samail ophiolite, Oman. *Earth Planet. Sci. Lett.* **144**, 435-451.

_____, _____ & GNOS, E. (1996): Rapid emplacement of the Oman: thermal and geochronologic constraints. *Tectonics* **15**, 1230-1247.

HERBOSCH, E.W. (1968): La viridine et la braunite de Salm-Château. *Bull. Soc. belge Géol., Paléontol. Hydrol.* **76**, 183-202.

KICKMAIER, W. & PETERS, T. (1991): Chert-hosted manganese deposits in the Wahrah Formation: a depositional model. *In* Ophiolite Genesis and Evolution of Oceanic Lithosphere (T. Peters, A. Nicolas & R.J. Coleman, eds.). Proc. Ophiolite Conf. (Oman, 1990). Kluwer Akademic Publishers, Dordrecht, The Netherlands (647-674).

KLEMM, G. (1911): Über Viridine, eine Abart des Andalusites. *Notizbl. Ver. Erdk. Grossh. Geol. landes Darmstadt* **32**, 4-11 [referred to by Abraham & Schreyer (1975)].

KRAMM, U. (1973): Chloritoid stability in manganese rich low-grade metamorphic rocks, Venn–Stavelot Massif, Ardennes. *Contrib. Mineral. Petrol.* **41**, 179-196.

_____ (1979): Kanonaite-rich viridines from the Venn–Stavelot Massif, Belgian Ardennes. *Contrib. Mineral. Petrol.* **69**, 387-395.

LIPPARD, S.J., SHELTON, A.W. & GASS, I.G. (1986): *The Ophiolites of Northern Oman*. Blackwell Scientific Publications, London, U.K.

MEINHOLD, K. & FRISCH, T. (1970): Manganese-silicate-bearing metamorphic rocks from central Tanzania. *Schweiz. Mineral. Petrogr. Mitt.* **50**, 493-507.

ÖDMAN, O.H. (1950): Manganese mineralization in the Ultevis district, Jokkmokk, north Sweden. 2. Mineralogical notes. *Årsbok Sver. Geol. Under.* **44**, no. 2 (Ser. C Avhandl Uppsat 516).

PASSCHIER, C.W. & TRUOW, R.A.J. (1996): *Microtectonics*. Springer-Verlag, Berlin, Germany.

PRIDER, R.T. & WHEELER, H.W. (1960): Viridine from Mount Ragged, Western Australia. *Indian Mineral.* **1**, 42-47.

SEARLE, M.P. & MALPAS, J. (1980): Structure and metamorphism of rocks beneath the Semail ophiolite of Oman and their significance in ophiolite obduction. *Trans. Roy. Soc. Edinburgh, Earth Sci.* **71**, 247-262.

SMITH, G., HÅLENIUS, U. & LANGER, K. (1982): Low temperature spectral studies of Mn^{3+}-bearing andalusite and epidote type minerals in the range 30000–5000 cm^{-1}. *Phys. Chem. Minerals* **8**, 136-142.

SPEAR, F.S. (1993): *Metamorphic Phase Equilibria and Pressure – Temperature – Time Paths*. Mineralogical Society of America, Washington, D.C.

SUZUKI, J., BAMBA, T. & SUZUKI, Y. (1965): On the viridine–quartz schist from the Chiei area, Hidaka Province, Hokkaido. *Proc. Japan Acad.* **41**, 722-727.

VRANA, S., RIEDER, M. & PODLAHA, J. (1978): Kanonaite, $(Mn^{3+}_{0.76}Al_{0.23}Fe^{3+}_{0.02})^{[6]}Al^{[5]}[O/SiO_4]$, a new mineral isotypic with andalusite. *Contrib. Mineral. Petrol.* **66**, 325-332.